Available online at www.sciencedirect.com
ScienceDirect
Acta Materialia 55 (2007) 243–250
Acta MATERIALIA
www.actamat-journals.com

Calculation of rose diagrams

S.-L. Chen [a,*], J.-Y. Zhang [b], X.-G. Lu [b], K.-C. Chou [b,c], W.A. Oates [d], R. Schmid-Fetzer [e], Y.A. Chang [f]

[a] CompuTherm, LLC, 437 S. Yellowstone Dr., Madison, WI 53719, USA
[b] School of Materials Science and Engineering, Shanghai University, Shanghai, China
[c] Department of Physical Chemistry, University of Science and Technology Beijing, Beijing, China
[d] Institute for Materials Research, University of Salford, Salford M5 4WT, UK
[e] Institute of Metallurgy, Clausthal University of Technology, D-38678 Clausthal-Zellerfeld, Germany
[f] Department of Materials Science and Engineering, University of Wisconsin-Madison, 1509 University Avenue, Madison, WI 53706, USA

Received 7 May 2006; received in revised form 10 July 2006; accepted 13 July 2006
Available online 17 October 2006

Abstract

Rose diagrams are isothermal sections of multicomponent phase diagrams which show highly symmetric phase boundaries due to multiple demixing occurring in a single phase. They result from using a Gibbs energy which is symmetric in the component concentrations. The unique features of rose diagrams are discussed, in particular their dependence on the presence of degeneracy in the Gibbs energy. The implications of degenerate equilibria in the application of the phase rule are also discussed.

Keywords: Rose diagram; Phase diagram; Phase equilibrium; Multicomponent systems; Phase rule

1. Introduction

Phase diagrams with multiple miscibility gaps in the liquid phase are frequently encountered in organic liquids and are of considerable technological importance to the petroleum industry [12]. They are also encountered in metallic systems, e.g. in multicomponent monotectic alloys [14].

As early as 1908, van Laar [2,3] calculated, by hand, ternary phase diagrams which contain miscibility gaps. In the 1960s, Meijering [4] also calculated some ternary phase diagrams which contain miscibility gaps. Rose diagrams are a special type of isothermal section found in multicomponent phase diagrams containing miscibility gaps. The term is applied to those phase diagrams that not only have multiple miscibility gaps, but also possess an extra topological feature – the miscibility gaps are present as multiple, highly symmetric rose-like petals. They were discussed extensively in a qualitative manner from a topological viewpoint, by Morral and Gupta [5,6]. They also carried out the first quantitative calculation of ternary rose diagrams [9].

Miscibility gaps in binary systems are simpler to understand and calculate than those occurring in higher-order systems and have, naturally, received more attention. Okamoto [7] discussed a two-peak miscibility gap in binary systems, and Hillert [8] later presented a historic note on such a type of diagram. Morral et al. studied in detail the topological properties of multicomponent rose diagrams [5,6] and first calculated a real ternary rose diagram [9]. The petals in rose diagrams are phase boundaries of miscibility gaps. The highly symmetric rose diagrams result from using highly symmetric thermodynamic functions.

Rose diagrams have another claim to importance in that they provide an excellent testing ground for a software's ability to calculate stable phase equilibrium, since performing calculations within the region where multiple phase equilibrium from a single thermodynamic function form is very difficult. Recent developments in the algorithm used

* Corresponding author. Tel.: +1 608 274 1414; fax: +1 608 274 6045.
E-mail address: chen@chorus.net (S.-L. Chen).

1359-6454/$30.00
doi:10.1016/j.actamat.2006.07.025

for phase diagram calculation [10] have enabled the study of this special type of phase diagram. All the diagrams presented in the present paper were calculated using the Pandat software [11,13]. Pandat has the ability to find the global stable phase equilibria automatically, without having to provide initial values for a desired phase equilibrium, as it uses a global minimization algorithm.

This paper is concerned with the actual calculation of rose diagrams. Not only does studying them help in understanding the phase relationships in a phase with highly symmetric thermodynamic properties, but also they may have practical significance, as miscibility gaps are not rare in real alloy and slag systems [14]. It will be shown, by presenting some examples of calculated rose diagrams in ternary and quaternary systems, that multiple demixing and degeneracy of phase equilibria can occur for very simple settings of the parameters in the modeling equations. However, miscibility gaps in binary systems will be considered first, as many of the important features found in rose diagrams are already apparent in the binaries. Binary miscibility gaps provide the opportunity to discuss degeneracy and the phase rule, and thereby make the multicomponent rose diagrams less difficult to understand.

2. Binary systems

Binary alloy phase diagrams which contain miscibility gaps are fairly common. Examples are the Al–Zn, Cu–Pb and Fe–Cr systems. Some of these gaps occur in the liquid phase and others in the solid solution phases.

Throughout this paper, numbers are used to label the phase regions, '1' for a single phase region, '2' for a two-phase region, and so on. For each system to be discussed, the demixing of a single phase is considered. Fig. 1 is a familiar type of phase diagram in which only one miscibility gap is found. The excess Gibbs energy function G^{xs} ($=G - G^{ideal}$) of the phase used in the calculation of Fig. 1 is given by

$$G^{xs} = Lx_1x_2 \tag{1}$$

In the excess Gibbs energies for all the phase diagrams to be presented, a value for L of 20 kJ mol^{-1} is used. The equations which determine a binary critical point are derived in Appendix. The critical point of the miscibility gap shown in Fig. 1 occurs at $x_B = 0.5$ and 1203 K for this regular solution model.

If the excess Gibbs energy is changed from Eq. (1) to the following:

$$G^{xs} = Lx_1x_2[1 + (x_1 - x_2)^2] \tag{2}$$

The phase diagram shown in Fig. 2 is obtained and is now seen to show a three-phase equilibrium and two critical points. Okamoto previously calculated a diagram similar to this one [7]. Using the equations for a binary critical point in Appendix, the two critical points in Fig. 2 occur at temperature of 1804 K and compositions of $x_B = 0.1464$ and $x_B = 0.8536$, respectively.

It is possible to have more than two critical points in a binary system if the following expression is used for the excess Gibbs energy

$$G^{xs} = Lx_1x_2[0.5 + (x_1 - x_2)^4] \tag{3}$$

It can be seen in Fig. 3 that a three-peak miscibility gap appears when this expression is used. With this particular equation, the two symmetrical peaks close to the pure components have the same shape, while the other one in the middle has a smaller peak. The two symmetrical critical points occur at a temperature of 1337 K and compositions of 0.0706 and 0.9294, respectively, while the critical point for the middle miscibility gap occurs at a temperature of 601 K at the mid-composition.

In order to obtain symmetrical phase diagrams like those shown in Figs. 1–3, it is necessary that the excess Gibbs energy should not contain any odd number in the power of the term $(x_1 - x_2)$.

The most interesting feature in the miscibility gap phase diagram shown in Fig. 3 is the occurrence of the four-phase equilibrium, and some time is spent discussing this feature,

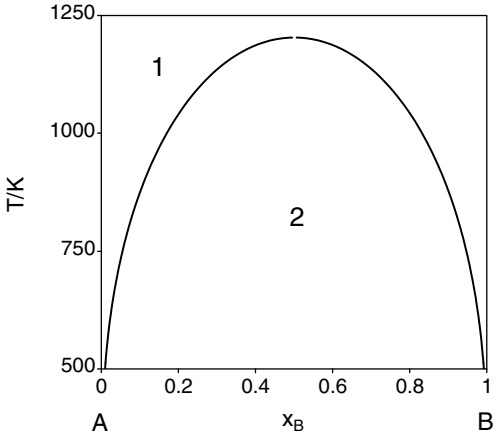

Fig. 1. A binary system with one miscibility gap. The phase fields are labeled according to the numbers of phases present.

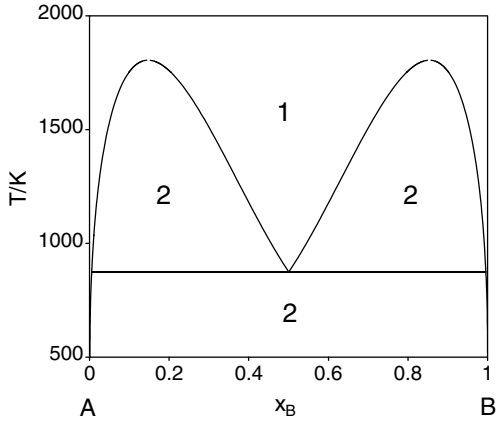

Fig. 2. A binary system phase diagram showing two miscibility gaps.

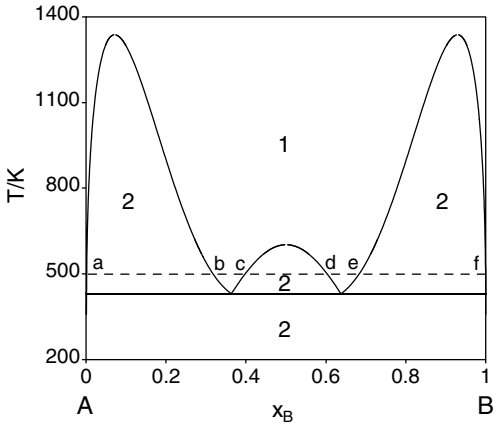

Fig. 3. A binary system phase diagram showing three miscibility gaps.

as analogous behavior is found in the multicomponent phase diagrams with miscibility gaps.

The reason for this apparent anomaly can best be appreciated by considering isotherms at 500 and 429.44 K (the invariant temperature) in Fig. 3. The Gibbs energy curves shown in Fig. 4 refer to these two temperatures, with the labeled points (a–f) in Figs. 3 and 4 for 500 K referring to the same compositions. It can be seen that, at the temperature above the invariant, there are three separate two-phase equilibria but that, at the invariant temperature they have merged to give the four-phase equilibrium. But this four-phase equilibrium itself consists of four separate degenerate three-phase equilibria.

The Gibbs' phase rule relates the number of degrees of freedom to the numbers of components and phases present in a system. It is usually stated, for fixed total pressure, as

$$F = C - \phi + 1 \tag{4}$$

where F, C and ϕ are the numbers of degrees of freedom, components and phases, respectively. This equation was derived by Gibbs from a consideration of systems in which only p–V work and chemical work were performed [1]. As soon as additional work forms are introduced, Eq. (4) must be modified, and a failure to do so will result in a violation of the phase rule if Eq. (4) is considered to be that rule. There are other situations where Eq. (4) is violated, and one arises in the case being considered here.

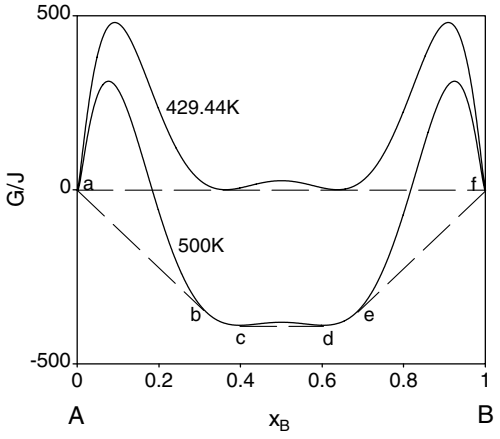

Fig. 4. Gibbs energies for the system shown in Fig. 3 at 500 and 429.44 K.

It can be seen from Eq. (4) that, for a binary system, the maximum number of coexisting phases is calculated to be three whereas, in Fig. 3, four phases clearly coexist at the invariant temperature. It is apparent then that, if Eq. (4) is considered to be the phase rule, there is a violation $F = -1$. The reason is that, in the derivation of the phase rule, Gibbs assumed that the phases were independent of each other. In fact, in the binary isobaric case, only three phases, represented by Gibbs energy curves shifting independently with temperature, may form a common tangent line at a unique temperature. The Gibbs energy of the fourth phase (or any additional phase) being tangent to the same line at exactly the same temperature must be mathematically dependent on the other phases. This is the case shown in Figs. 3 and 4 because of the high symmetry in the Gibbs energy function. The introduction of any asymmetry into the excess Gibbs energy expression, Eq. (3), would, of course, immediately remove the degeneracy, producing truly separate three-phase equilibria. It is possible to revise Gibbs' phase rule by explicitly considering the number of independent phases or Gibbs–Duhem relations, but this will not be elaborated here.

3. Ternary systems

The features of rose diagrams are not seen in binary temperature–composition diagrams. In order to observe them, isothermal sections must be considered in higher-order systems. Ternary isoplethal sections also have some interesting properties but will not be discussed here.

Morral and Davis [9] calculated a simple ternary rose diagram. Two examples of ternary rose diagrams are presented here, and some interesting features in rose diagrams are revealed. In the first ternary example, the binary system parameters previously used in the calculation of Fig. 2 have been selected for the three binary systems, and a Redlich–Kister–Muggianu extrapolation of these terms is used for the calculation of the ternary system's properties. Symmetrical rose petals in the ternary isothermal diagram are encouraged if a ternary interaction term is also introduced. The excess Gibbs energy expression used for the ternary phase and resulting in the diagrams shown in Fig. 5 is given by

$$G^{xs} = L\{x_1x_2[1 + (x_1 - x_2)^2] + x_2x_3[1 + (x_2 - x_3)^2] + x_3x_1[1 + (x_3 - x_1)^2] + 2.5x_1x_2x_3\} \tag{5}$$

In order to visualize how the phase relationships change with temperature, isothermal sections at temperatures of 1073, 1173, 1273, 1293, 1308 and 1423 K were calculated and are shown in Fig. 5. At 1073 K, the central region is a three-phase region. When the temperature increases to 1173 K, the single phase becomes stable in the center of

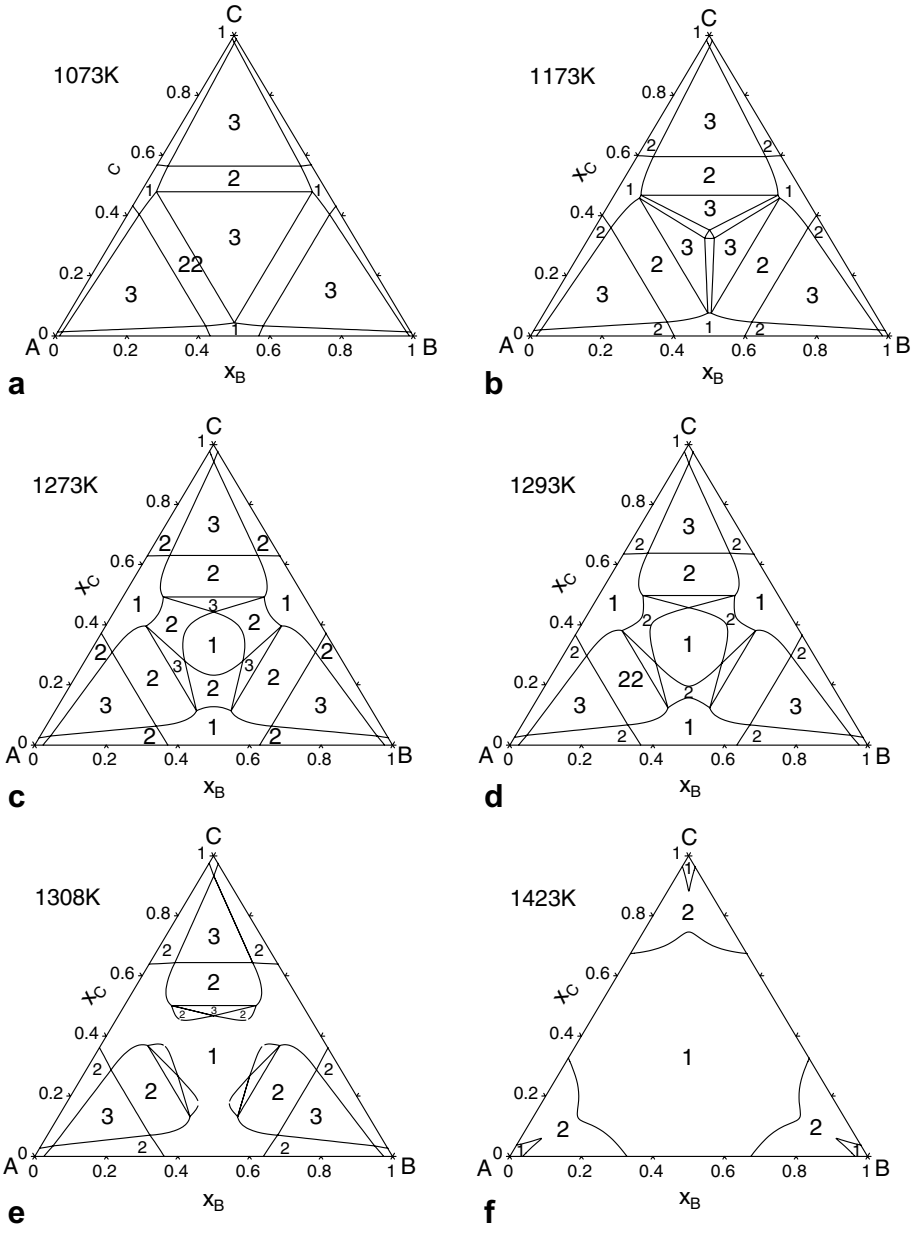

Fig. 5. Ternary isothermal sections of the phase diagram at different temperatures for a phase described by Eq. (5).

the compositional triangle, and then rose-like diagrams appear at 1273 and 1293 K. With a further increase in temperature, the rose diagram splits into three parts, giving 'radish' diagrams, as shown at 1308 K in Fig. 5e. The miscibility gaps gradually become smaller with increasing temperature and, as seen in Fig. 5f for 1423 K, the three-phase equilibria vanish. The miscibility gaps completely disappear at the binary critical temperature of 1804 K in Fig. 2.

In the second ternary example, the excess Gibbs energy is given by

$$G^{xs} = L\{(x_1x_2 + x_2x_3 + x_3x_1) + 4x_1x_2x_3\} \quad (6)$$

In this representation, the binaries are assumed to be regular, and there is just a single ternary interaction term. Unusual behavior is observed in that, at temperatures which are just above the binary critical points, the rose petals face towards the edges of the compositional triangle (see Fig. 6a), while at higher temperatures they face the corners of the triangle (see Fig. 6b). An intermediate temperature range exists for the transition between the two types of rose diagrams shown in Fig. 6a and b. As shown in Fig. 6c and d, a hexagonal-shaped region is found in the central region, and this is surrounded by six two-phase miscibility gaps. Fig. 7 shows a perspective view of the Gibbs energies along the phase boundaries of the diagram shown in Fig. 6c and d with the lobes in this figure being the Gibbs energies along the two-phase envelopes shown in those figures. The Gibbs energy values at the hexagonal-shaped six-phase region can be seen to be constant owing to the degeneracy. Each of the six phases is in equilibrium with each other, generating a

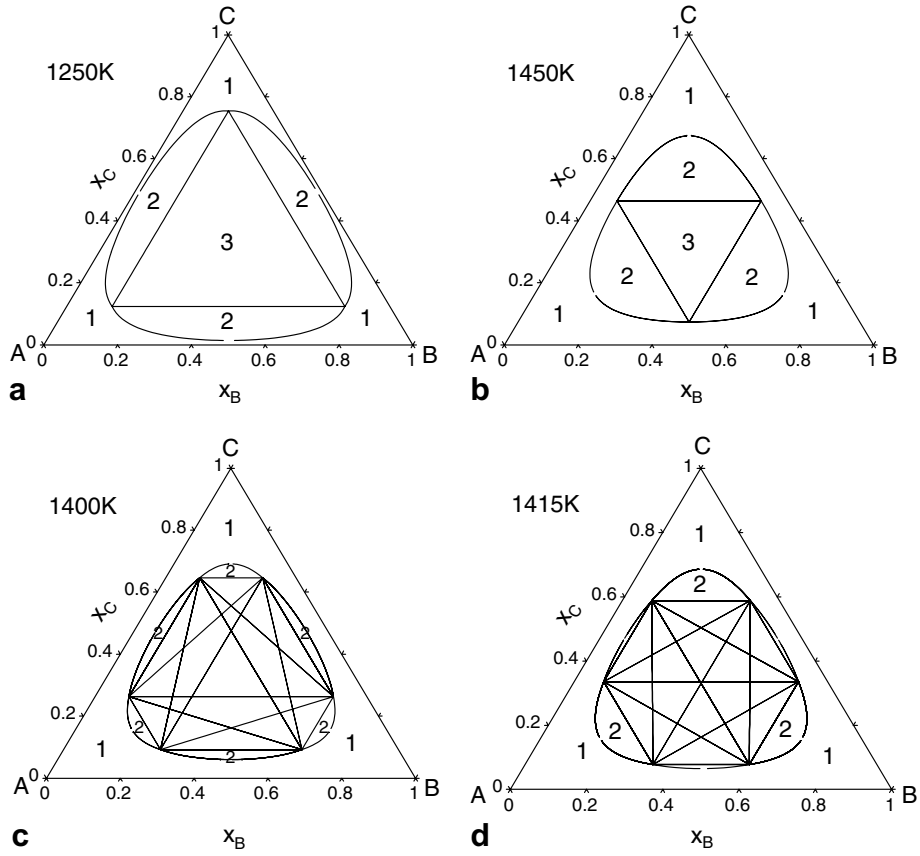

Fig. 6. Ternary isothermal sections of the phase diagram at different temperatures for a phase described by Eq. (6).

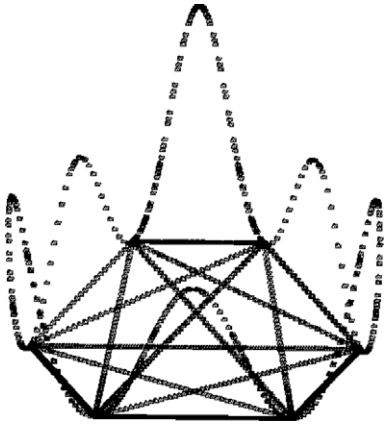

Fig. 7. Perspective view of the Gibbs energies along the phase boundaries in a system similar to that shown in Fig. 6c and d. The hexagonal shaped Gibbs energy surface produces 15 tie-lines and 20 different degenerate three-phase tie triangles.

total of 15 tie-lines, shown in Fig. 6c and d. It is in fact the space enclosed by the 15 tie lines generating the six-phase equilibrium area which, in this case, also involves 20 three-phase tie triangles derived from the six different phases. The fact that some of the 15 tie-lines cross each other is not unusual but is also observed in any non-degenerate ternary invariant transition type reaction among four phases.

Since this topology persists over a small transition temperature range, the degeneracy is univariant. A stable equilibrium calculation for an alloy with equal concentrations of the three components clearly reveals the transition shown in Fig. 6a and b. Fig. 8 shows the relationship of the phase fractions–temperature for this equiatomic alloy. Below 1380 K, only one three-phase tie-triangle exists, and the three phases have the same phase fraction for this system

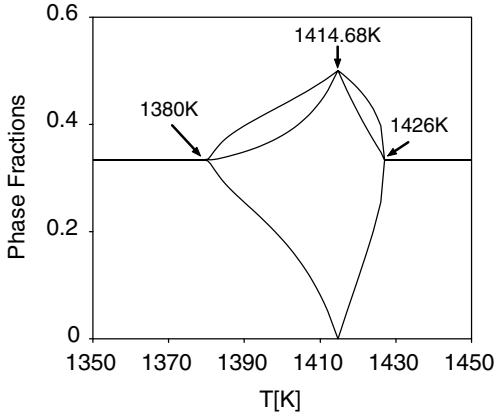

Fig. 8. Phase fractions vs. temperature diagram for equal compositions of components in a system at the center of the Gibbs triangle corresponding to the ternary in Fig. 6 demonstrating the univariant transition range.

with equal compositions, as seen in Fig. 6a. Above 1426 K, another type of just one three-phase tie-triangle exists until it disappears at a much higher temperature. Between these two temperatures is a transition temperature range, at which the six-phase hexagon exists, as shown in Fig. 6c and d. Within this transition temperature range, the calculated phase fractions of the three phases are not equal. At 1414.68 K, two phases have the same phase fraction of 0.5, while the other one has zero fraction, as a regular hexagon happens only at this particular temperature. Only at this temperature does a tie-line pass through the overall composition, thus enabling the partition in two phases with equal fraction. There are actually three different tie-lines passing through the center point, enabling the distribution to any of the six phases at their end points. Here it is noted that Fig. 8 shows only one of the limiting cases. In order to enhance readability, the fractions are shown for three phases only when tracing the course of the three-phase triangle from Fig. 6a to b. If one of the two symmetric (equilateral) three-phase triangles in Fig. 6c had been picked for tracing, the phase fractions would have been constant and equal to 1/3 in the entire transition range. Between 1380 and 1426 K, any infinite number of combinations of fractions of the six coexisting phases marked by the vertices of the hexagon is actually a possible equilibrium state, provided the fractions comply with the materials balance. Thus, Fig. 8 shows the phase fractions for any of the smallest triangles enclosing the overall composition; its upper curve also marks the upper limit of any attainable phase fraction in the transition range.

The central hexagonally shaped areas in Fig. 6c and d indicate that, for this univariant situation, there are six phases in equilibrium. But if Eq. (4) is used, with $C = 3$ and $\phi = 6$, it is found that $F = -2$. The reason is again that the Gibbs energy functions of the six phases visualized by the six lobes in Fig. 7 are not independent. The high symmetry of the simple Eq. (6) produces this mathematical dependency and, thus, the degeneracy of the phase equilibria. This is analogous to the binary example discussed earlier.

4. Quaternary systems

In the first quaternary example, the excess Gibbs energy is expressed by

$$G^{xs} = 0.25L\{x_1x_2 + x_1x_3 + x_1x_4 + x_2x_3 + x_2x_4 + x_3x_4 + 10[x_1x_2x_3 + x_2x_3x_4 + x_1x_2x_4 + x_1x_3x_4] + 100x_1x_2x_3x_4\} \quad (7)$$

Four different sections of diagrams calculated using this expression at different temperatures and with different compositions of one component are shown in Fig. 9. In reading these quaternary diagrams, it is noted that straight lines are generally only given as boundaries of four-phase equilibria. This is because an isothermal four-phase equilibrium forms a tetrahedron in composition space, and the four corners are the coexisting single-phase points. If the quaternary phase diagram section at $x_D = \text{constant}$ happens to cut off only one corner of this tetrahedron, the resulting four-phase field must be a triangle. If the quaternary section cuts off two corners of the tetrahedron, the resulting four-phase field must be a quadrilateral (see Fig. 9a and d). Since the faces of the tetrahedron are three-phase equilibria, it becomes clear that the borders of the four-phase triangles or quadrilaterals must be straight lines, each corresponding to a section of a different three-phase equilibrium. A special case arises when the four-phase tetrahedron degenerates to a quadrilateral.

The diagrams in Fig. 9 have high symmetry. An interesting feature in these diagrams is that six phases can coexist over some temperature range ~773 K. Each of the six phases is close to the middle of a binary edge; in Fig. 9a and b, at 773 K, one phase with 46.4 at.% A, 46.4 at.% B, 3.6 at.% C and 3.6 at.% D is close to the A–B edge and so on for all six edges. In the quaternary compositional space at constant temperature, these six phases form an octahedron inside the composition tetrahedron. This octahedron consists of 15 different tetrahedra, in which three of them degenerate to squares. Partial overlapping exists among the 15 tetrahedra. This is analogous to Fig. 6c and d, where six single-phase points can form up to 20 different tie-triangles. Two 2D sections at 773 K are given in Fig. 9a and b. As shown in Fig. 9b, the regular hexagon is formed from those four-phase equilibria with the constraint $x_D = 0.25$. Another feature is found when the isothermal section changes from the composition $x_D = 0.25$. Fig. 9a is a section with $x_D = 0.2$. The regular hexagons separate, and an extra triangle forms in the center. However, the central triangle is a part of the three larger triangles of four-phase equilibria. Fig. 9a shows the 15 sectioned tetrahedra, which are partially overlapping (three small triangles, three large triangles, six parallelograms and three lines).

Compared with Fig. 9a–c, Fig. 9d is a diagram enlarged to show the detail of the phase regions at 1873 K. An interesting feature can be seen from Fig. 9b–d. Only one four-phase region exists at the middle temperature (1073 K). At lower (873 K) and higher (1873 K) temperatures, more than one four-phase region is found. It is expected, therefore, that many more complicated phase relationships in multicomponent rose diagrams will be found.

Finally, the most rose-like diagram of all is presented in Fig. 10. The excess Gibbs energy for this phase is described by an equation which has no binary interaction terms

$$G^{xs} = L\{5[x_1x_2x_3 + x_2x_3x_4 + x_1x_2x_4 + x_1x_3x_4] + 2.5x_1x_2x_3x_4\} \quad (8)$$

In the center of the rose diagram is a hexagon comprising seven four-phase regions. Two layers of petals surround the hexagon. The inside layer has six three-phase regions, and the outside layer six two-phase regions. The two layers are connected by six small groups of phase regions, each of

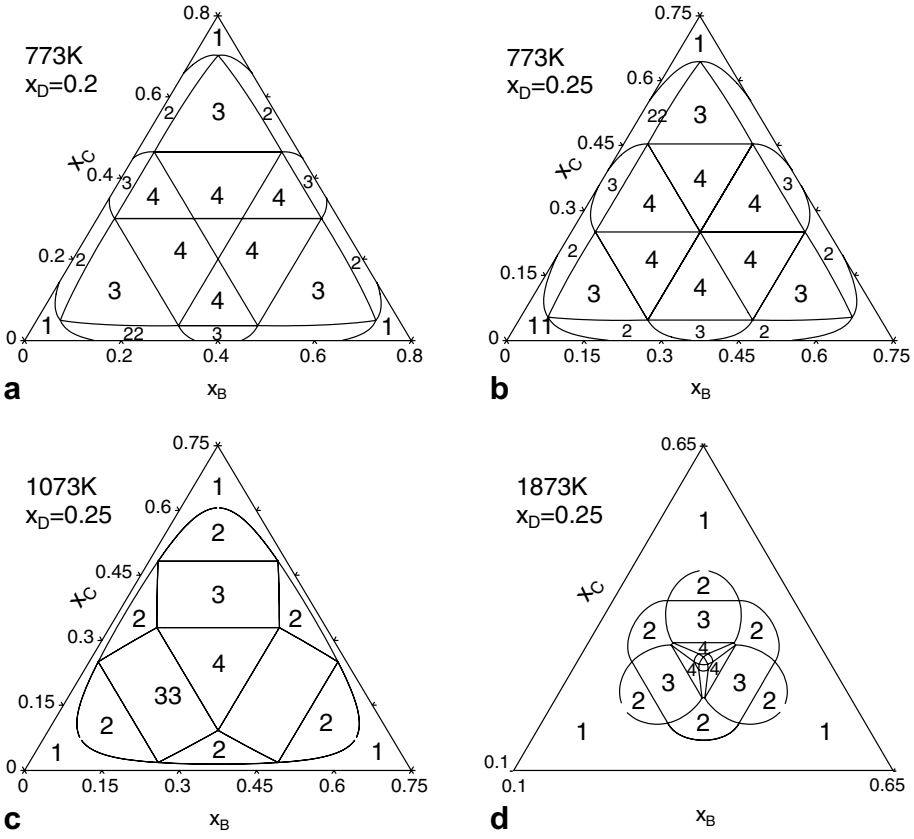

Fig. 9. Quaternary isothermal sections at different temperatures for a phase described by Eq. (7). (a) $x_D = 0.2$, (b–d) $x_D = 0.25$.

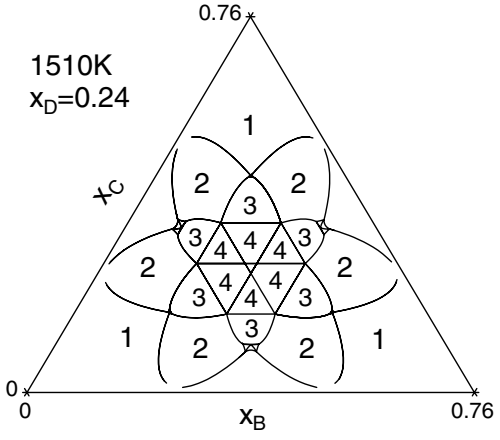

Fig. 10. A rose diagram in a quaternary system with the phase described by Eq. (8).

them has one two-phase, two three-phase and one four-phase. All these phase regions together form this special rose diagram.

5. Discussion and summary

Some of the extremely rare phase relationships presented, such as the presence of a four-phase equilibrium in a binary system at constant pressure, can only happen in hypothetical systems. Although the phase relationships obtained from using excess Gibbs energies of high symmetry may not appear in real systems, they can help us understand related phase equilibria in multicomponent systems.

Calculation of these rose diagrams puts great demands on the software's ability to find the stable phase equilibrium automatically, since it is difficult to guess and supply initial values for finding the stable equilibria. The presence of degeneracy also makes the calculation of rose diagrams particularly difficult. The results reported here have depended on the use of the global minimization algorithm implemented in Pandat [10].

Some examples of rose diagrams in multicomponent systems have been presented to illustrate the geometrical symmetry of the rose-like diagrams. Careful adjustment of the parameters in the excess Gibbs energy can produce a lot of different patterns of the phase relationships. Rose diagrams show high geometrical symmetry and are found in some isothermal sections of phase diagrams and are the consequence of the symmetry in the Gibbs energy equations used. Degeneracy of the invariant equilibria also results from the high symmetry, and the phase rule must be applied with care to these situations. The usual statement for the constant total pressure phase rule $F = C - \phi + 1$ is violated for these cases involving degenerate equilibria.

Acknowledgements

S.L.C. thanks Shanghai University for their invitation and support in the summer of 2005. K.C.C. expresses his thanks to the Ministry of Education of China and the National Science Foundation of China for their financial support under Contract Nos. 2002-0210-550 (EDU), 50274008 (NSFC), 2002-0212-860 (NSFC). R.S.F. thanks the German Research Foundation (DFG) for support in the Priority Program 'DFG-SPP 1120: Phase transformations in multicomponent melts' under Grant No. 588/24. Y.A.C. thanks the financial support from the Air Force of Scientific Research (AFOSR Grant No. F49620-03-1-0083) and the Wisconsin Distinguished Professorship.

Appendix. Critical point for miscibility gaps in binary systems

$$G = G^{\circ} + G^{\mathrm{id}} + G^{\mathrm{xs}} \tag{A1}$$

$$G^{\circ} = x_1 G_1^{\circ} + x_2 G_2^{\circ} \tag{A2}$$

$$G^{\mathrm{id}} = RT(x_1 \ln x_1 + x_2 \ln x_2) \tag{A3}$$

$$G^{\mathrm{xs}} = x_1 x_2 \sum_{i=0}^{m} L_i (x_1 - x_2)^i \tag{A4}$$

The necessary conditions for the critical point are

$$\begin{cases} \frac{\mathrm{d}^2 G}{\mathrm{d}x_2^2} = 0 \\ \frac{\mathrm{d}^3 G}{\mathrm{d}x_2^3} = 0 \end{cases} \tag{A5}$$

where x_2 is chosen as the dependent compositional variable, and x_1 depends on x_2. The derivatives for Eqs. (A2)–(A4) are given below.

$$\frac{\mathrm{d}^2 G^{\circ}}{\mathrm{d}x_2^2} = \frac{\mathrm{d}^3 G^{\circ}}{\mathrm{d}x_2^3} = 0 \tag{A6}$$

$$\frac{\mathrm{d}G^{\mathrm{id}}}{\mathrm{d}x_2} = RT(-\ln x_1 + \ln x_2) \tag{A7}$$

$$\frac{\mathrm{d}^2 G^{\mathrm{id}}}{\mathrm{d}x_2^2} = RT\left(\frac{1}{x_1} + \frac{1}{x_2}\right) \tag{A8}$$

$$\frac{\mathrm{d}^3 G^{\mathrm{id}}}{\mathrm{d}x_2^3} = RT\left(\frac{1}{x_1^2} - \frac{1}{x_2^2}\right) \tag{A9}$$

$$\frac{\mathrm{d}G^{\mathrm{xs}}}{\mathrm{d}x_2} = (x_1 - x_2) \sum_{i=0}^{m} L_i (x_1 - x_2)^i - 2x_1 x_2 \sum_{i=1}^{m} i L_i (x_1 - x_2)^{i-1} \tag{A10}$$

$$\frac{\mathrm{d}^2 G^{\mathrm{xs}}}{\mathrm{d}x_2^2} = -2 \sum_{i=0}^{m} L_i (x_1 - x_2)^i - 4(x_1 - x_2) \sum_{i=1}^{m} i L_i (x_1 - x_2)^{i-1} + 4x_1 x_2 \sum_{i=2}^{m} i(i-1) L_i (x_1 - x_2)^{i-2} \tag{A11}$$

$$\frac{\mathrm{d}^3 G^{\mathrm{xs}}}{\mathrm{d}x_2^3} = 12 \sum_{i=1}^{m} i L_i (x_1 - x_2)^{i-1} + 12(x_1 - x_2) \sum_{i=2}^{m} i(i-1) L_i (x_1 - x_2)^{i-2} - 8x_1 x_2 \sum_{i=3}^{m} i(i-1)(i-2) L_i (x_1 - x_2)^{i-3} \tag{A12}$$

References

[1] Gibbs JW. Trans Connecticut Acad 1875–1876(October–May): 108–248.
[2] van Laar JJ. Z Phys Chem 1908;63:216.
[3] van Laar JJ. Z Phys Chem 1908;64:257.
[4] Meijering JL. Philips Res Rep 1963;18:318.
[5] Morral JE, Gupta H. Scripta Met 1991;25:1393–6.
[6] Morral JE, Gupta H. J Chim Phys 1993;90:421–7.
[7] Okamoto H. J Phase Equil 1993;14:336–9.
[8] Hillert M. J Phase Equil 1994;15:35–6.
[9] Morral JE, Davis RH. J Chim Phys 1997;94:861–8.
[10] Chen S-L, Daniel S, Zhang F, Chang YA, Oates WA, Schmid-Fetzer R. J Phase Equil 2001;22:373–8.
[11] Chen S-L, Daniel S, Zhang F, Chang YA, Yan X-Y, Xie F-Y, et al. CALPHAD 2002;26:175–88.
[12] Sadus RJ. High pressure phase behaviour of multicomponent fluid mixtures. Amsterdam: Elsevier; 1992.
[13] Chen S-L, Zhang F, Daniel S, Xie F-Y, Yan X-Y, Chang YA, et al. J Met 2003;55(12):48–51.
[14] Groebner J, Schmid-Fetzer R. J Met 2005;57(9):19–23.